Designing an Updated System for Time Lapse Microscopy to Study *Toxoplasma Gondii* Invasion in Intestinal Epithelial Cells

A Technical Report submitted to the Department of Biomedical Engineering

Presented to the Faculty of the School of Engineering and Applied Science
University of Virginia • Charlottesville, Virginia

In Partial Fulfillment of the Requirements for the Degree
Bachelor of Science, School of Engineering

Alexa Guittari
Spring, 2021

Technical Project Team Members
Carolyn Graham
Danielle Heckert
Sydney McMahon

On my honor as a University Student, I have neither given nor received unauthorized aid on this assignment as defined by the Honor Guidelines for Thesis-Related Assignments

Signature _____ Date _May 8th, 2021_
Alexa Guittari

Approved _____ Date _____
Brian Helmke, Department of Biomedical Engineering

Designing An Updated System for Time Lapse Microscopy to Study *Toxoplasma gondii* Invasion in Intestinal Epithelial Cells

By

Carolyn Graham, Department of Biomedical Engineering
Alexa Guittari, Department of Biomedical Engineering
Danielle Heckert, Department of Biomedical Engineering
Sydney McMahon, Department of Biomedical Engineering
Advisor: Brian Helmke, Department of Biomedical Engineering

Designing An Updated System for Time Lapse Microscopy to Study *Toxoplasma gondii* Invasion in Intestinal Epithelial Cells

Carolyn Graham[a], Alexa Guittari[a], Danielle Heckert[a], Sydney McMahon[a], Brian Helmke[a,1]

[a] Department of Biomedical Engineering, University of Virginia, Charlottesville, VA
[1] Correspondence: helmke@virginia.edu, MR4 1124 Charlottesville, VA 22908, 434-924-6460

Abstract

Toxoplasma gondii is a parasite that infects about a third of the global population and can cause the disease toxoplasmosis. While the infection does not cause toxoplasmosis for most people, the disease can cause life threatening complications for immunocompromised individuals, who are more likely to contract the disease. This group includes people with inflammatory bowel disease (IBD) who suffer from extreme discomfort and debilitation due to irregular peristalsis. A relationship exists between *T. gondii* invasion of epithelial cells and the impaired gut motility of those with IBD, potentially contributing to the increased susceptibility to toxoplasmosis for people with IBD. In order to study this relationship, a stretch device and environmental chamber are needed to mimic peristalsis and to provide physiological conditions while stretching. Thus, the primary aim of this project was to design an environmental chamber that enabled the observation of cell stretching via time lapse microscopy. Engineering concepts were utilized to design this environmental chamber, which was then fabricated through laser cutting and 3D printing. The stretch device allowed the study of cell morphological adaptation changes when presented with the external mechanical stimulus (i.e. stretching to mimic peristalsis). The overall intention of the project was to set up the fundamentals so that one could study the morphological features of host cells and how they relate to *T. gondii* invasion. While the environmental chamber was not produced in time for use on the microscope, data from cell stretching showed that the change in circularity of cells were 14.93% and 10.5% for biaxial stretch and uniaxial stretch respectively, which is evidence that cells do demonstrate phenotypic changes after being stretched to mimic peristalsis.

Keywords: Toxoplasmosis, Inflammatory Bowel Disease, Mechanobiology, Stretch-adaptation

Introduction

Toxoplasma gondii is an extremely common parasite that is known to chronically infect roughly 33% of the world's population[1]. In fact, as many as 14% of Americans are seropositive for *T. gondii* by age 40[2]. The high prevalence of the parasite is due to the fact that it can invade and replicate in almost all of the nucleated cells in warm blooded animals[1]. Interestingly, the chronic infection of *T. gondii* typically does not result in any symptoms for immunocompetent individuals as the healthy immune system is able to successfully attack the parasitic infection. However, if the parasite is able to successfully invade the host's tissues and escape detection by the immune system, the individual experiences a series of severe symptoms resulting from the infection, which is also referred to as toxoplasmosis.

Successful invasion occurs through a series of four steps: contact, attachment, penetration, and invasion. First, an important structure referred to as the moving junction forms between the apical tip of the parasite and the host cell membrane[1]. The parasite is then able to penetrate into the cell by exploiting the actomyosin motor system of the host cell. As invasion continues, *T. gondii* forms a parasitophorous vacuole within the host cell. However, the biomechanics behind *T. gondii* invasion in immunosuppressed individuals is still unclear, as it is not known fully understood which steps of the invasion process make the cells especially susceptible to toxoplasmosis.

One subset of immunosuppressed patients who are at an increased risk of developing toxoplasmosis

are those with inflammatory bowel disease (IBD). IBD is an umbrella term for Crohn's disease and ulcerative colitis, both of which affect peristalsis, the involuntary muscular contraction and relaxation of the gut that moves a bolus of food down the intestinal tract[3]. Importantly, the exact relationship between *T. gondii* invasion and stretch adaptation of cells due to peristalsis is unclear. While it is known that the gut epithelial cells in patients with IBD have a distinct, cobblestone-like appearance that is unlike the normal, columnar shape, it is not clear how this contributes to the increased susceptibility of *T. gondii* invasion [4,5]. The causality of this relationship has not yet been established. One hypothesis is that the irregular peristaltic movements prevent the epithelial cells in IBD patients from becoming stretch-adapted, which could play a role in making IBD individuals more susceptible to contracting toxoplasmosis. It is also possible that toxoplasmosis alters the cell shape, as Apicomplexan parasites such as *T. gondii* have been seen to alter gastrointestinal motility[6]. This understanding is immensely important for the field as it has the potential to elucidate more effective treatment options for patients suffering from both IBD and toxoplasmosis.
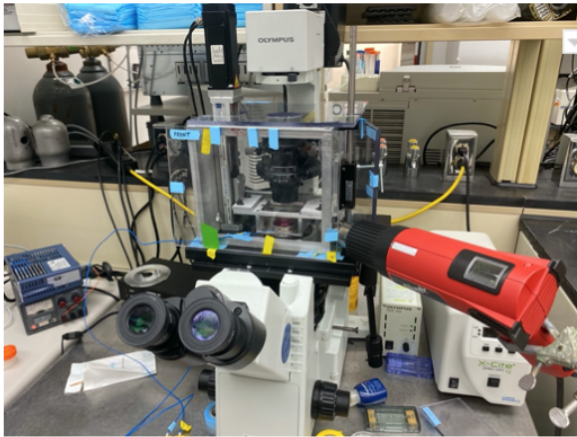
Therefore, the aim of this project was to investigate the relationship between the enhanced susceptibility to toxoplasmosis and the altered cell morphology in IBD patients via time lapse microscopy. In order to do this, a stretch device system that mimicked peristalsis while simultaneously simulating cellular physiological conditions was needed. This device would be used to perform cell stretch experiments to elucidate *T. gondii* invasion mechanisms on both healthy, stretched-adapted and diseased, non-stretched cells.

The original stretch device system consisted of the stretch device and an environmental chamber. The chamber, as seen in Figure 1, is composed of four plexiglass panels held together with tape, and a heat gun that directly heats the interior of the chamber. The panels fit around the stretch device and on the microscope stage.
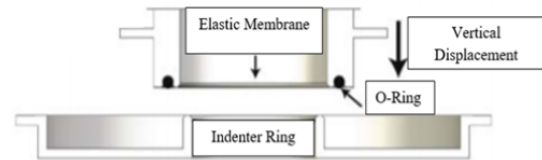

Figure 2: Membrane holder ring and indenter ring cross section. *This cross section shows the elastic membrane where cells are plated held in the membrane holder ring (MHR) by a silicone O-ring. The motor controls the vertical displacement of the MHR; a negative vertical displacement causes the membrane to stretch over the intenter ring. Image reproduced from ref. 7 with permission from the authors.*

Figure 1: Current stretch device system. *The above setup shows the stretch device placed on the microscope stage, surrounded by the four plexiglass panels taped together that make up the environmental chamber. The red heat gun is placed in an opening between panels to control the temperature of the cells. This setup is not conducive to producing accurate results.*

Shown in Figure 2 is the stretch device as originally designed by Huang et al[7]. The device consists of a linear actuator and motor that control the upward and downward movements of a mobile plate that holds a membrane holder ring (MHR) with a polydimethylsiloxane (PDMS) membrane on which cells are cultured[7]. When the MHR passes over the indenter ring, as seen in Figure 2, the membrane and cells are stretched. This stretching is what mimics the contractile movements of the intestine.

There are several limitations to this system that the team sought to fix with an updated chamber design. First, the chamber was designed and built for use on a DeltaVision RT Restoration Microscope and thus is not compatible with the Olympus IX51 Inverted Fluorescence Microscope that future experiments will be conducted with. Additionally, the positioning of the heat gun focuses too much heat on some areas of the PDMS membrane, which results in an uneven distribution of heat within the cell plate. There is also no mechanism to measure humidity levels in the chamber. Furthermore, setting up the current environmental chamber and maintenance of consistent physiological conditions takes 1-2 hours, which causes inconveniences and delays during experiments. Lastly, the device does not protect the microscope from the toxic parasite used in experiments, *T. gondii*, if leakage onto the microscope plate were to occur.

The additional aim for this project was to obtain lab data that would allow us to gain a better understanding of how *T. gondii* interacts with stretched intestinal epithelial cells. The team hoped to examine the mechanisms by which *T. gondii* invades epithelial cells and how this process differs between stretch-adapted and non stretch-adapted cells. These experiments would be done using the stretch device and environmental chamber to simulate peristalsis in physiological conditions.

Results

Environmental Chamber

The first step in the design process of a novel device involved taking measurements of the Olympus IX51 Microscope in the lab. Once these measurements were made, drawings of a chamber from these specifications were made in AutoDesk Fusion, a computer-aided design (CAD) program. The design process consisted of three major iterations of the chamber (Figure 3). The first iteration, shown in Figure 3A, was of a five-sided chamber design that was based on the current four-panel set up and measurements. The second iteration, shown in Figure 3B, modified the design to make the dimensions more accurate in response to the acquisition of additional photographs and measurements of the original setup, and included the removal of the bottom panel, allowing the chamber to rest on the microscope stage. The final iteration, shown in Figure 3C, came as a result of a consultation with Dr. William Guilford, an expert on biological design fabrication methods. Dr. Guilford recommended various changes that would better account for the logistical constraints, fabrication limitations, and consider the assembly process of the chamber onto the microscope.

The final design shown in Figure 4 involves five pieces, some that are laser cut and some that are 3D printed to be assembled on the microscope. All of the clear pieces are acrylic and were laser cut, and the orange and white pieces were 3D printed
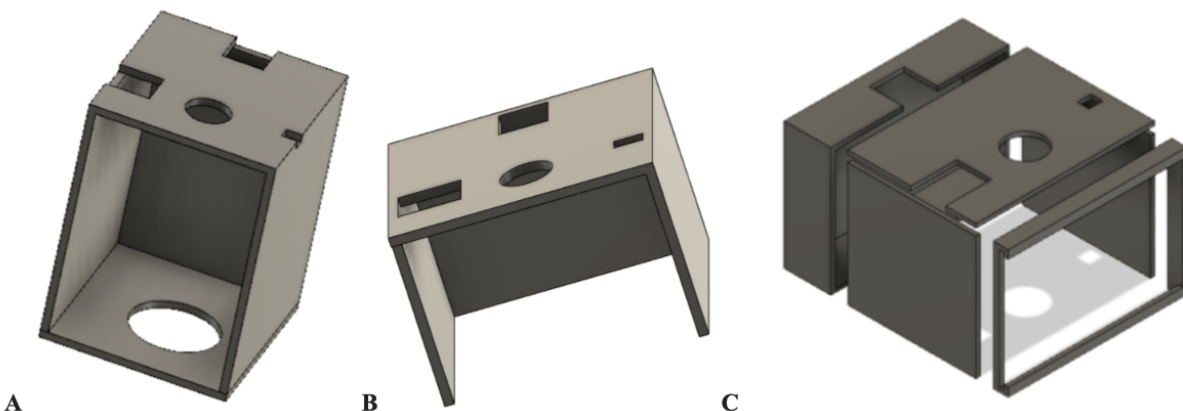

Figure 3: Iterations of the environmental chamber design. *The three panels show the iterations of our CAD drawings of the environmental chamber. (A) Panel A shows the first iteration, which has five sides, including a bottom piece. (B) Panel B shows the bottom piece removed, as it was deemed unnecessary. (C) Panel C shows the final design, which was split into five individual pieces for laser cutting and 3D printing.*
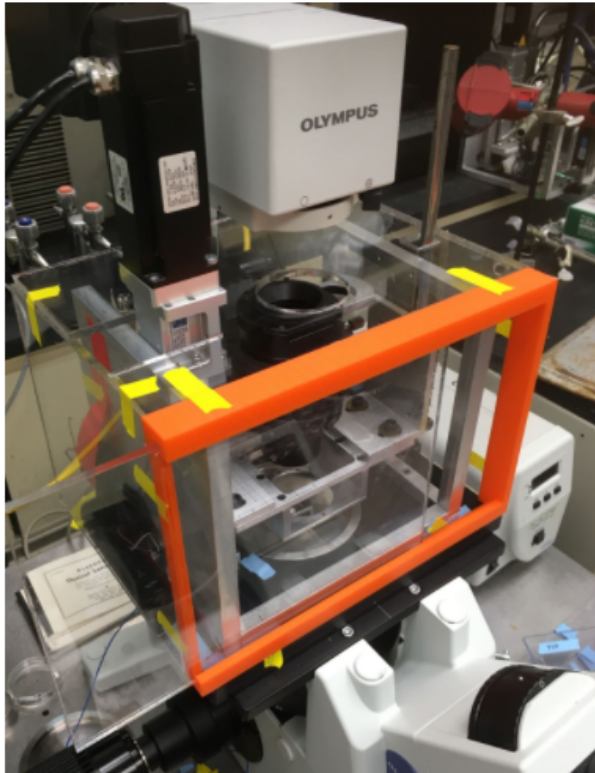
Figure 4: Assembled final chamber design. *The above setup shows the novel environmental chamber design, assembled onto the microscope stage surrounding the stretch device. The back piece is not included in this assembly since it did not fit.*

due to their complexity. There is a sliding panel in the front of the chamber to allow for access to the MHR and microscope stage as needed during experimentation and handling. While the pieces could easily be glued together in the future, they are still attached using tape for now to allow for future modifications to individual pieces until the device is fully optimized, especially since the back piece did not fit as planned. Heating pads will be ordered in the future that adhere to the two side panels and the back piece once the device design is further optimized. Time constraints prevented the team from conducting validation tests, but the team was still able to assemble the environmental chamber onto the microscope, and it is on track to be very useful for mimicking physiological conditions in order to conduct a variety of cell stretch experiments, including future experiments to assess *T. gondii* invasion in intestinal epithelial cells.

Stretch Experiments
Microbead Stretch
As was mentioned previously, stretching cells on PDMS membranes while using the computer-controlled stretch device created by Huang et al. allows for peristalsis to be mimicked and produces results that demonstrate phenotypic changes in the cells related to stretch[7]. Prior to stretching cells, PDMS membranes containing microbeads were stretched to determine whether the stretch device was applying strain equal to the strain expected to be applied, to confirm that the stretch device was working as expected. This was done by measuring the distance L_0 between two beads before stretch, and the distance L between two beads after stretch, calculating strain for each pair, and then averaging this strain for multiple pairs of beads. Equation 1 was used to calculate the strain, ε.

$$\text{Equation 1: } \varepsilon \; = \; \frac{L-L_0}{L_0}$$

The average calculated strain was 0.007, whereas the stretch device was set to apply a strain value of 0.10. The difference between these two measurements can be explained by the fact that L and L_0 were measured by hand and only one image was available with which to perform these calculations. This also led to the strain decreasing in one location, while increasing in others, which would suggest the stretch device was not entirely working as expected. Therefore, future experimentation should include additional strain measurements to see if this was a small error or a larger problem with the stretch device. Due to COVID-19 limitations, the group was unable to obtain additional overlaid images to measure the strain that was being applied by the stretch device, and fully confirm that the actual strain was equal to the applied strain.

Cell Stretch
After stretching the microbeads to ensure that the stretch device was calibrated and properly functioning, the PDMS membranes with both microbeads and human foreskin fibroblasts (HFF-2s) were stretched. The original environmental chamber and stretch device system was used in all of these cell stretch experiments due to the time constraints posed by the fabrication
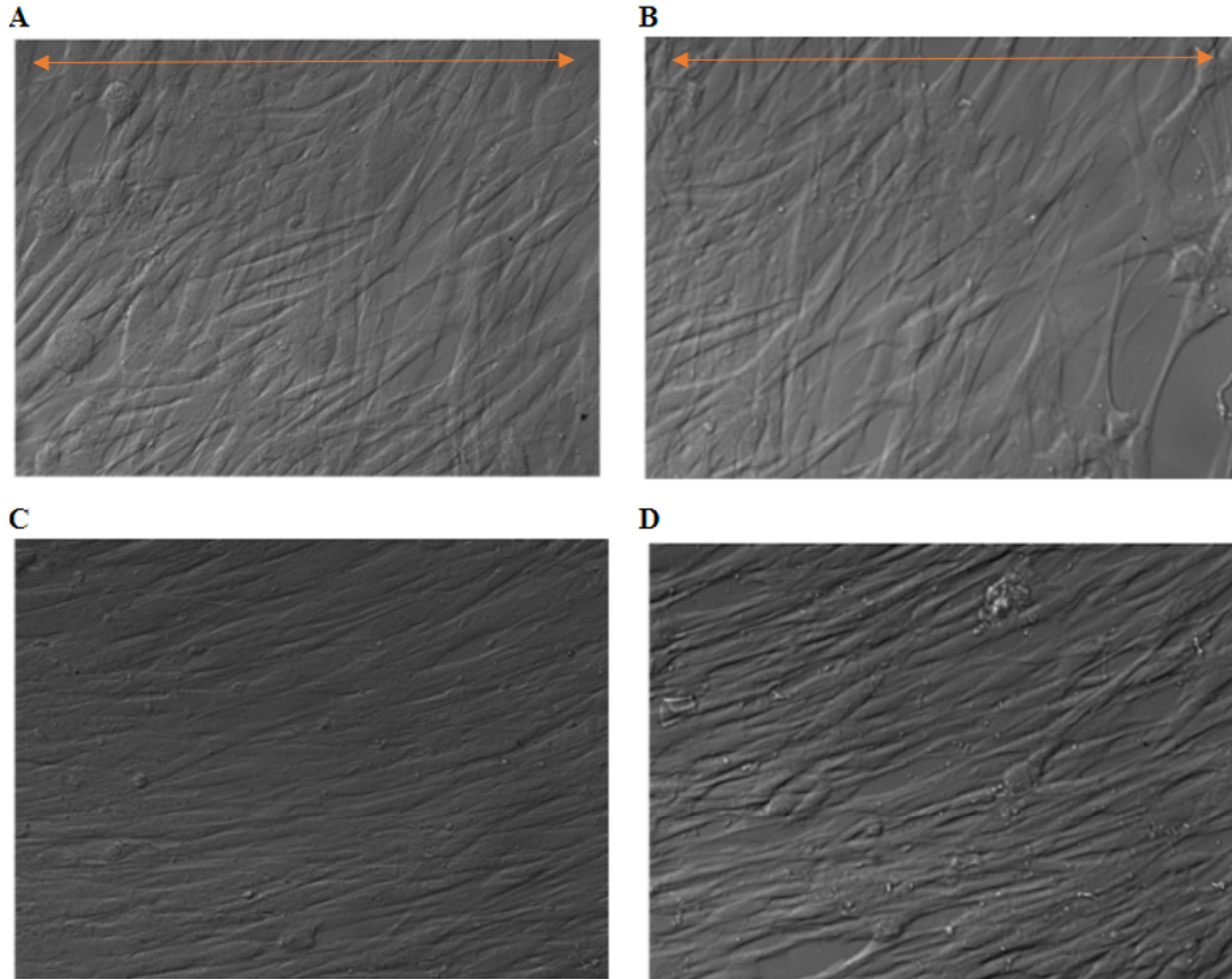
Figure 5: Effects of cell stretching. *The four images show cells before and after uniaxial and biaxial stretching. (A) Image A shows cells before stretching, (B) Image B shows these same cells after uniaxial stretching. The cells were stretched to the left and the right for uniaxial stretching, as is indicated by the arrows. (C) Image C shows cells before stretching, (D) Image D shows these same cells after biaxial stretching.*

process for developing a new chamber. Cells were stretched uniaxially to determine if they respond to stretch, and then other cells were stretched equi-biaxially to mimic peristalsis, as seen in Figure 5. ImageJ was then used to analyze the cell morphology after stretching. Circularity, a metric representing how circular a shape is relative to a perfect circle was used to measure the morphological changes using Equation 2 [8]. For uniaxial stretch, shown in Figure 5A and Figure 5B, the average circularity increased 10.5%, and for biaxial stretch, shown in Figure 5C and Figure 5D, the average circularity after stretch increased 14.9% relative to before stretch.

Equation 2: $Circularity = \frac{4\pi A}{p^2}$

ImageJ was also used to measure the area, perimeter, and solidity of the cells. The solidity, which is a comparison of convex cell area relative to concave cell area, describes the stiffness and deformation of cells, such that high solidity values indicate fewer membrane protrusions, which is important for cell migration[8]. The solidity and circularity before and after stretch were calculated by averaging measurements of the shapes of cells for each stretch type, then calculating circularity and solidity from these averages. The percent

changes for solidity and circularity reflect the changes after stretch relative to before stretch. For uniaxial stretch, shown in Figure 5A and Figure 5B, the average solidity increased 1.0%, and for biaxial stretch, shown in Figure 5C and Figure 5D, the average solidity increased 1.4%.

pH Measurements
The pH of the cells needed to be measured before and after experimentation to ensure that a pH around the physiological pH of 7.4 was maintained. HEPES (4-(2-hydroxyethyl)-1-piperazineethanesulfonic acid) buffer was added to the cell culture media for this purpose. This buffer served to ensure that the pH stayed within the desired range of physiological conditions, with minimal variance, throughout the stretch experiments. The pH of the cell culture media containing HEPES was then measured before and after stretching cells with the stretch device. A paired t-test with four degrees of freedom, due to the five different trials, was performed to determine whether the pH stayed constant from the beginning of the experiments until the end. The pH readings were taken four separate times for each trial and then averaged, with the t-test being conducted using these averages. A p-value of 0.015 was obtained, indicating that the pH was significantly different at the $\alpha = 0.05$ significance level after stretch as compared to before stretch.

Discussion
Interpretation of Cell Experiment Results
For the microbead stretching, the original intent was to use an interactive data language (IDL) particle tracker to track the movement of the beads. The alternative that was used was measuring the distance the bead traveled which was calculated using ImageJ. The distance traveled was measured by the center of the bead for equi-biaxial stretch only. This measurement is used to determine the strain magnitude on the membrane. Due to time constraints, the team was unable to obtain stretch images of microbeads for uniaxial stretch, so the results only reflect biaxial stretch. Results were not obtained pertaining to the efficacy of the new stretch system using the newly designed environmental chamber due to time constraints, so there are no further results necessitating interpretation.

Significance and Innovation of the Project
The new chamber creates a suitable environment in which the biomechanics of parasitic invasion can be accurately studied. With the original system that lacked an adequate environmental chamber, it was impossible to ensure that the results produced were valid for the physiological conditions that exist in the human intestinal tract. The novel chamber developed as part of this Capstone will permit research to be conducted under conditions closer to those within the human body once the chamber is fully optimized.

Furthermore, the downstream research performed with this environmental chamber has the potential to elucidate novel therapeutics for toxoplasmosis in patients with IBD. The primary treatment option currently available for toxoplasmosis is pyrimethamine and sulfadiazine plus folinic acid; however, this treatment has been shown to only be effective in 60-70% of patients [9]. These treatment protocols were developed primarily through cell biology approaches, whereas therapeutics based on mechanobiology have been minimally studied. Therefore, this environmental chamber has the downstream potential to revolutionize toxoplasmosis therapies for patients with IBD by taking an approach focused on mechanobiology.

Limitations
As a result of the ongoing COVID-19 pandemic, the team experienced delays and complications getting into the lab. In fact, in mid-March only one team member was allowed in the lab, and it was not until the beginning of April that the rest of the group was permitted to enter. Thus, the preliminary lab steps were delayed as the team was not able to calibrate the instruments or perform initial testing until the second half of the Spring semester. Because most of the time spent in the lab was dedicated to prerequisite work, the team was unable to perform experiments using *T. gondii*. As a result, the team was not able to test the hypothesis regarding the relationship between enhanced susceptibility to toxoplasmosis and cell phenotype for people with IBD.

Furthermore, all initial cell experiments were conducted using HFF-2s, although the original plan was to use human intestinal epithelial cells which would more accurately mimic peristalsis

since these are the cells found in the human intestinal tract. Human intestinal epithelial cells also take longer to culture, which was a limiting factor due to the small time period during which the team was permitted to be in the lab. Additionally, handling human intestinal epithelial cells requires the implementation of new protocols, which would have further postponed the beginning of the experimental process. Therefore, the team had to assume that any results obtained via experimentation with HFF-2s would sufficiently translate to intestinal epithelial cells, but this assumption should be reconsidered for future experimentation.

Additionally, the delayed entry to the lab space posed a challenge for printing the environmental chamber because the team was not able to acquire the necessary measurements of the microscope until mid-March. This heavily impacted the design iterations because without a precise understanding of the microscope and stretch device, it was difficult to design the chamber accordingly. COVID-19 limitations also delayed access to the fabrication facilities. Therefore, a printed prototype of the device was not produced until April 30, thus preventing testing of the chamber to assess its validity and preventing further iterations of the design process for the chamber that will be needed to fully optimize it. Consequently, cell experiments could not be performed using the novel chamber and all results presented earlier were obtained via the original stretch device system. The team therefore had to make the assumption that the results would be similar, but more representative of physiological conditions when the newly designed chamber is fully integrated into the system.

Finally, limitations associated with the 3D printer affected the final design. As mentioned earlier, the team chose to 3D print the back of the environmental chamber due to the level of detail involved; however, the specifications and limitations of the printer results in slight deformities of this piece. Additionally, some components of the microscope were not accounted for, such as the width of the microscope arm and the presence of electrical cords along the microscope arm. Therefore, future modifications will be necessary so that the dimensions of this piece are modified to better fit the microscope arm while also allowing space for the cords that run along the arm. Future iterations of the prototype should consider other fabrication methods, such as laser cutting, for this component of the device to prevent deformation from occuring again.

Implications for Future Research and Considerations

Future work on this project may include further developing the design of the environmental chamber to include more sensors for gas and humidity regulation, to include microscope protection from the parasite, to optimize the materials used, and to optimize the chamber's fit on the microscope. Additionally, given that the limitations of 3D printing introduced unforeseen deformities into the prototype, future work could look to remedy this issue, perhaps by using different fabrication techniques. Throughout the design iteration process, experimental testing would be needed to confirm physiological conditions are met as needed. Changes would then be implemented as necessary.

Once these tests and modifications are completed, the team hopes the relationship that was intended to be elucidated between *T. gondii* invasion and host epithelial cell phenotype can be found. Replicating the stretch experiments with the new environmental chamber to make sure the results are consistent will also be important. Therefore the team hopes that future stretch experiments such as those completed by this team can be conducted using the new chamber, both to further test the consistency of results using the new system, and to develop a greater understanding of how cells, specifically intestinal epithelial cells, stretch in response to peristaltic-like movements. Further research should therefore use intestinal epithelial cells, instead of the HFF-2s that have been used so far.

Building on these initial stretch experiments, future teams can perform work with *T. gondii* and observe in detail its initial interactions with the host cell. Further research may include invasion assays which would measure the quantity of the parasite that invades a host cell in a specific time period. The parasite could be fluorescently-tagged to permit the observation of this quantification.

Furthermore, one can study different host cell lines and their phenotype as they adapt to physiological conditions of applied mechanical stimuli, not just peristaltic movement. The long term goal is to eventually be able to understand and predict what the parasite looks for in order to carry out invasion. Through identification of cell characteristics that the parasite targets, future teams can develop a therapeutic to block this interaction and ultimately stop the parasite from invading.

Additionally, computational modeling should be considered in the future. This method could elucidate novel findings regarding the cell stretch dynamics, as modeling would eliminate human lab error. Computational modeling will also allow researchers to have a deeper and more accurate understanding of the *T. gondii* invasion process in a quicker and more efficient way. Modeling would allow researchers to automate the analysis process, consequently allowing for the generation of larger sets of data in a more efficient manner.

The team researched and reviewed literature on computational models relating to *T. gondii* invasion and cell stretching, and discovered a potentially relevant model titled "Kinetic Modeling of *Toxoplasma gondii* Invasion"[10]. In this model, Kafsack et al. uses a compartmental modeling approach in R programming language that includes five stages of invasion. The model requires experimental data in order to model *T. gondii* invasion, so data collected with future lab experiments could be used to run this model and explore various aspects of *T. gondii* invasion computationally. Therefore, future researchers could utilize a combination of this model and agent-based modeling to create a system that would facilitate the analysis of *T. gondii* invasion.

Materials and Methods
Chamber Design
The design of the chamber resulted from researching previous models and comparing them to the current stretch device in the lab. Regarding this prior art, there are already several stretch device systems on the market, some of which incorporate environmental chambers and some of which do not. Two companies, CuriBio and FLEXCell, have promising stretch devices - the

Cytostretcher and inverted StageFlexer, respectively - that can be used for cell stretching experiments similar to those to be carried out with *T. gondii* [11,12]. However, these cell stretching systems have limitations. The limitations for the StageFlexer include using a vacuum as the stretch system, which is a less precise and harder control way of stretching cells. The limitations for the Cytostretcher include the high cost of the product, and the limited stretch profile options; this device only allows for uniaxial stretch which does not mimic peristaltic movements.

The stretch device currently in the lab was determined to be the best option for stretch devices because it has the ability to stretch in both biaxial and uniaxial profiles. Uniaxial stretch is important for calibrating the device so that it can be ensured that cells are indeed stretching. Biaxial stretch as mentioned above is what mimics the contractile movements of the intestine known as peristalsis[13]. Additionally, the original device enables frequency calibration monitored by a computer. While this device has the stretching capabilities needed for experiments, the major limitation was a lack of an environmental chamber to mimic physiological conditions while performing time lapse microscopy.

Based on this research, and a knowledge of the limitations of the original system used in the lab, a list of desired criteria were developed for the ideal cell stretch system. It was essential that the system allowed for high microscope resolution to properly image the cells and that it provided microscope protection and easy cleanability to protect against *T. gondii*. Additionally, in order to ensure the accuracy of our experiments, the system had to be able to mimic and support physiological conditions such as temperature, pH, and gas concentrations. Furthermore, the ideal chamber would be easy to set up and clean in order to facilitate the experimentation process.

It was determined that these criteria could be adequately met if an effective environmental chamber was used to supplement the original system as designed by Huang et al [7]. While there are other environmental chamber options on the market such as microscope incubators, the high cost of these solutions limits their potential

viability, and they possess some of the same limitations as did the CuriBio and FLEXCell cell stretching systems.
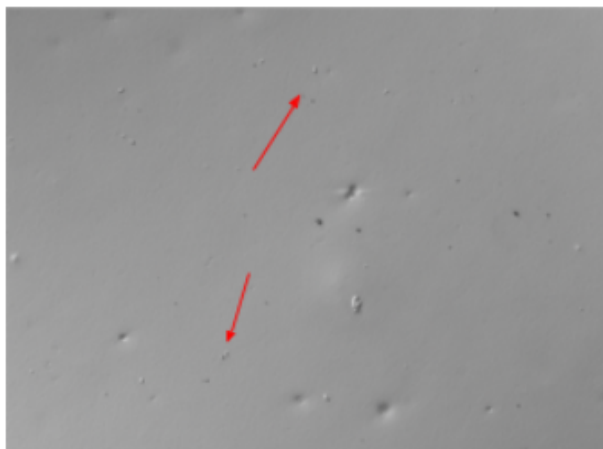

Figure 6: Imaged microbeads prior to stretch. After serial dilutions were performed to obtain the correct number of microbeads per field of view (5-10 microbeads), the membrane was imaged and was ready to stretch. This image shows the correct number of microbeads per field of view.

Based on this initial research, we created a concept selection matrix, shown in Supplementary Table 1, to more easily weigh the benefits and drawbacks of each major design option. The criteria for our design were determined based on the goals of experiments and the time and resources available, as well as design requirements discovered in the preliminary research. The leftmost column of Supplementary Table 1 contains these design criteria, with the second column weighing each criteria based on its relative importance. For each design option, we ranked each criterion such that a five represents the most desirable option for the criterion, and a one represents the least desirable option for that criterion. These values were determined based on knowledge of various types of chambers and their pros and cons, and predictions as to how each design option would satisfy each criterion. These values were added together to obtain a final score out of five for each design option. Based on the highest total scores, the selected design option was a mountable environmental chamber using a heat jacket as the heat source. Initially, the intention was for this to

be a water jacket, but after further consideration a heat jacket made of heating pads was selected instead, since a water jacket was determined to be a more complicated option than heating pads.

Preparation of the PDMS Membranes
Imaging of both microbeads and cells required the assembly of PDMS membranes. The initial preparation steps are the same for both. PDMS membranes and rubber O-rings, which hold the PDMS membrane in the MHR, were sonicated in 70% ethanol for fifteen minutes. The PDMS membranes and O-rings were taken out of the sonicator and dried until the ethanol was completely evaporated. The membrane was then properly aligned in the MHR and the O-ring was securely inserted into a grove to hold the membrane in place.

Microbead Plating
Once the PDMS membranes were prepared as explained above, microbeads needed to be plated on the membranes. 1.5μL from a microbead stock solution was added to 1mL of 100% ethanol and sonicated for five minutes. These microbeads are fluorescently tagged in order to measure the distance between their movement before and after stretch without the concern of their lifespan. 1μL of this solution was then taken out and added to another 1mL of 100% ethanol and sonicated again. This dilution process was repeated two more times, after which 1mL was placed on a PDMS membrane. The serial dilution was performed to obtain a proper amount of beads per field of view. Figure 6 shows the correct number of microbeads per field of view, approximately 5 to 10 microbeads. The membrane was then left to dry overnight to then be stretched and imaged the following day.

PDMS Membrane Coating for Cells
After preparing PDMS membranes as mentioned above, further preparation for plating cells was done. 3mL of 0.1N NaOH was added onto these membranes for 30 minutes, followed by three five-minute washes of 5mL of distilled H2O. Then 2mL of 3% APTES was added on each membrane for 20 minutes, followed by three five-minute washes of 5mL distilled H2O. Next, 2mL of 1% glutaraldehyde was added for 30 minutes, and three five-minute washes of 5mL distilled H2O

followed. To make the collagen that is added next to the membrane, 66μL of collagen (Collagen I rat tail, Cat No: A10483-01, Lot No: 1325202) was added to 1967μL of 0.02M acetic acid. The collagen mixture was then filtered with a 0.22μm filter and 2mL of this was then plated onto one PDMS membrane, followed by 4℃ refrigeration overnight. The following day, three five-minute washes with DPBS +/+ was done on the membrane and then it was sterilized for 60 minutes under the UV in the biosafety cabinet (BSC).

Cell Inoculation and Plating
HFF-2s were thawed and inoculated for experimentation in a T-25 flask. Once the HFF-2s were 100% confluent, the T-25 flask was taken out of the incubator. The existing cell growth media was aspirated and 5mL of PBS -/- was added to the flask. This was removed after a gentle stirring around the flask and 1mL of trypsin was added. The flask was incubated for two minutes. Next, 7.5mL of growth media was added and everything was transferred to a 15mL centrifuge tube which was centrifuged at 250 RMG for five minutes. The liquid was aspirated, leaving the cell pellet that formed from centrifugation. 5mL of growth media was added and the pellet was broken up. Then this mixture was placed on a hemocytometer to count and average the number of cells. Equation 3 was used to figure out how many cells/mL to plate on a membrane.

Equation 3:
$$cells\ per\ mL\ to\ plate\ =\ \frac{2.85E5\ cells/mL}{avg.\ \#\ cells\ counted*10^4}$$

Growth media was then added in an amount of 6mL minus the number of mL of cells present. This media containing cells were then plated on top of the membranes. The membrane was placed back in the incubator for 1-2 days to settle and grow. Immediately prior to stretching, the growth media was aspirated and 6mL of a stock solution of growth media and HEPES (25mL growth media plus 625μL HEPES) was added. The cells were then ready to be stretched.

Stretch Device Set Up
Prior to performing any stretch experiments, the device needed to be set up, which included checking that the device frequency was accurate,

making sure the cell media would not evaporate once stretching began and making sure the heat gun provided appropriate physiological temperature. Additionally, the pH meter machine needed to be calibrated prior to cell stretch.

Oscilloscope
The oscilloscope measures the frequency of the linear actuator and motor that is part of the stretch device as seen in Figure 7. Prior to performing any stretch experiments, it was confirmed that the stretch device was operating at a frequency of 0.15Hz. The calibration measurements were calculated using the oscillation from the stretch device. The stretch device was performing a frequency of 0.153Hz which indicates that more adjustments need to be made to obtain the 0.15Hz frequency since its period was 0.1538 seconds.
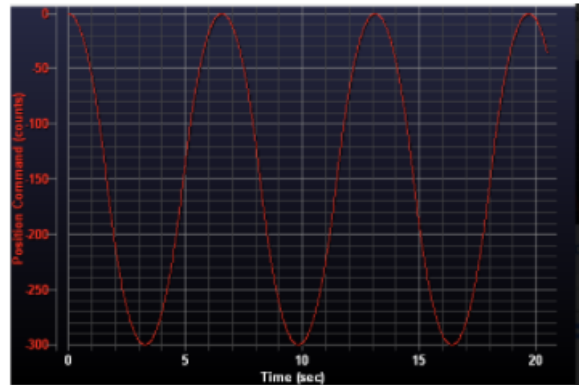

Figure 7: Oscilloscope reading. *This is the graph of the oscillation from the stretch device moving from position zero, its starting point, to its highest position of 300 units. The frequency of the stretch device was calculated to be 0.153Hz.*

Evaporation Trials
Evaporation trials were done on the microscope stage while the stretch device and environmental chamber with the heat gun were set up. These trials were done to test how much liquid would evaporate due to the heat gun to mimic the cell media evaporation during cell stretch experiments. The first evaporation trial consisted of putting a 60mm petri dish with a lid containing water in the environmental chamber with the heat gun set up for thirty minutes. Some evaporation did occur. In order to measure the evaporation, a black line was marked where the top of the water originally was and checked after thirty minutes to see if the water

dropped below the black line. The next trial that was done consisted of the same set up but with parafilm around the petri dish; not as much water dropped below the black line. As a result, it was determined that cell stretch trials could be run. In the future more trials should be repeated to more fully ensure that the cell media does not evaporate.

Temperature

The heat gun served as the original temperature control for cell stretch experiments. Initially a thermometer was used to measure the temperature and was placed on the stage of the microscope, but this setup did not accurately reflect the temperature experienced by the cells, so thermocouples were bought to be taped near the MHR to gain more accurate temperature readings. The position of the heat gun was adjusted several times to observe how heat travels within the environmental chamber. Since some parts of the chamber were hotter in other places based on the thermocouple readings, we chose the best location to account for this and to keep a constant temperature of 37℃. Using the thermocouple, it was determined that the initial temperature at this location was 37℃, then 35.9℃ after 15 minutes, and finally 38.8℃ after 45 minutes. These values were all within a reasonable range of 37℃, such that experiments could be conducted. However, the new chamber design aims to keep this temperature much closer to 37℃ than was shown here. For the purposes of the initial experiments, however, once the heat gun was set in the appropriate position and the thermocouples read 37℃, the cells could be added to the stretch device to be stretched.

pH Meter Calibration

Measurements of the pH were taken using a pH meter machine. Calibrations of the device were done using known pH buffer solutions of 4.0, 7.0, and 10.0. An electrode was used to obtain a pH reading for the buffer solution and cell media mixtures.

Stretching Microbeads and Cells

Microbead Stretch

In order to ensure that the stretch device was exerting an equal amount of strain onto the membrane, microbeads were stretched prior to cells. The beads were stretched in a biaxial

direction to most similarly mimic the physiological conditions of peristalsis [13,14]. The stretch device is set at a starting position of 0 where the membrane is touching the indenter ring. The motor then moves the stretch device down and up by 300 units, so that the first motion stretches the membrane over the indenter ring and ends at position 300. The return motion moves back up 300 units to the starting position where the membrane is flush with the indenter ring.
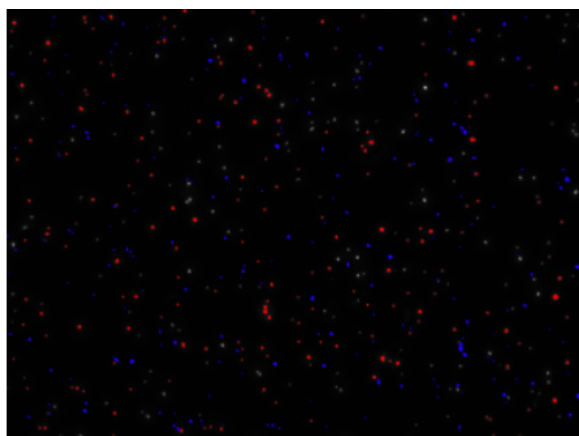

Figure 8: Overlaid microbead images. *Three microbead images obtained during stretch were overlaid. The white beads were imaged prior to stretch, at position zero, the red beads were imaged at the highest position during stretch and the blue beads were imaged upon return to position zero.*

After stretching we measured the distance between beads to see if the distances were the same as before stretching. To calculate the distances for stretch, an overlaid image was applied as seen in Figure 8. The beads labeled in white were imaged before stretch. The beads in red are the beads when maximally stretched to a position of 300 units. The beads labeled in blue represent the position of the beads when the stretch device returns to the starting position. The white and blue beads do not perfectly overlap, potentially due to image registration errors, since the blue beads were all approximately 5.96 pixels away from the corresponding white beads, all in the same direction. While the stretch device moves 300 units below position zero and 300 units back up to position zero over the course of stretch experiments, the user must manually stop the stretch device at position zero to image after stretch. Because of this manual stopping, the final

position is not guaranteed to be precisely at position zero, meaning it does not stop at exactly the same position that the MHR started at. This can prevent the intended overlap between the white and blue microbeads.

Cell Analysis

Cells were imaged before and after the stretch experiments. ImageJ was used to analyze the cells before and after stretch using the trace tool within the program. The tool was used to obtain an algorithm of an ellipse to permit the application of the best fit ellipse equation. This equation allows for the evaluation of changes in circularity, which represent how cell morphology changes[8].

End Matter

Author Contributions and Notes

C.J.G, A.A.G, D.B.H and S.G.M designed research, C.J.G, A.A.G, D.B.H and S.G.M performed research,, C.J.G, A.A.G, D.B.H and S.G.M analyzed data; and C.J.G, A.A.G, D.B.H and S.G.M wrote the paper. The authors declare no conflict of interest.

References

1. Kato, K. How does *Toxoplasma gondii* invade host cells? *J. Vet. Med. Sci.* **80**, 1702–1706 (2018).

2. Furtado, J. M., Smith, J. R., Belfort, R., Gattey, D. & Winthrop, K. L. Toxoplasmosis: A Global Threat. *J. Glob. Infect. Dis.* **3**, 281–284 (2011).

3. Fakhoury, M., Negrulj, R., Mooranian, A. & Al-Salami, H. Inflammatory bowel disease: clinical aspects and treatments. *J. Inflamm. Res.* **7**, 113–120 (2014).

4. Booth, C. C. Enterocyte in coeliac disease. 1.

Br. Med. J. **3**, 725–731 (1970).

5. Bharucha, A. E., Camilleri, M., Low, P. A. & Zinsmeister, A. R. Autonomic dysfunction in gastrointestinal motility disorders. *Gut* **34**, 397–401 (1993).

6. Halliez, M. C. M. & Buret, A. G. Gastrointestinal Parasites and the Neural Control of Gut Functions. *Front. Cell. Neurosci.* **9**, (2015).

7. Huang, L., Mathieu, P. S. & Helmke, B. P. A stretching device for high-resolution live-cell imaging. *Ann. Biomed. Eng.* **38**, 1728–1740 (2010).

8. Hart, M. L. *et al.* Shaping the Cell and the Future: Recent Advancements in Biophysical Aspects Relevant to Regenerative Medicine. *J. Funct. Morphol. Kinesiol.* **3**, 2 (2018).

9. Wang, Z.-D. *et al.* Toxoplasma gondii Infection in Immunocompromised Patients: A Systematic Review and Meta-Analysis. *Front. Microbiol.* **8**, (2017).

10. Kafsack, B. F. C., Carruthers, V. B. & Pineda, F. J. Kinetic modeling of Toxoplasma gondii invasion. *J. Theor. Biol.* **249**, 817–825 (2007).

11. Pasapera-Limon, A. M. *et al.* Application of Cyclic Uniaxial Stretch: New Tools for Understanding the Role of the Extracellular Matrix in Cell Biology. 7 (2018).

12. Colombo, A., Cahill, P. A. & Lally, C. An analysis of the strain field in biaxial Flexcell membranes for different waveforms and frequencies. *Proc. Inst. Mech. Eng. [H]* **222**, 1235–1245 (2008).

13. Terry, B. S., Lyle, A. B., Schoen, J. A. & Rentschler, M. E. Preliminary Mechanical Characterization of the Small Bowel for In Vivo Robotic Mobility. *J. Biomech. Eng.* **133**, 0910101 (2011).

14. Gravesen, F. H., Funch-Jensen, P., Gregersen, H. & Drewes, A. M. Axial force measurement for esophageal function testing. *World J. Gastroenterol. WJG* **15**, 139–143 (2009).

Supplementary Figures

Criteria (1-5)	Weight	Chamber Size			Heat Source		
		Large	Small	Mountable	Heat gun	Heat jacket	Lightbulb & Glass
Setup time	0.1	3	3	3	3	3	4
Heating time	0.1	2	5	5	1	5	4
Cost	0.1	5	3	4	5	4	3
Uniform airflow	0.05	2	3	3	1	3	3
Uniform heat	0.1	2	5	4	1	5	4
Evaporation risk	0.1	4	2	2	1	5	5
pH measurement ease	0.05	5	4	4	0	0	0
Customizability	0.1	2	4	5	4	4	4
Design simplicity	0.1	5	3	4	4	2	3
Microscope protection	0.1	4	5	4	0	0	0
Microscopy quality	0.1	3	4	5	4	5	5
Totals	1	3.35	3.75	3.95	2.35	3.45	3.35

Supplementary Table 1: Concept selection matrix. A mountable chamber size and a heat jacket heat source were selected due to these design options having the highest total scores.